Final Project
Galaxy Luminosity Function-II. Observations vs Simulations

Yingtian Chen *†‡

December 6, 2020

Abstract

The luminosity function (LF) is a straight forward measurement, observationally. However, when speaking about simulations, the LF is no longer easy to get. Various works have tried to reproduce the LF in simulations but get limited achievement due to insufficient resolution and lack of knowledge of the sub-grid physics. In this work, I take advantage of one of most state-of-art cosmological simulations, IllustirsTNG, to provide the halo mass function, galaxy luminosity function, and the star formation efficiency of the FOF/SUBFIND catalogs of halos/subhalos. I find that median and small size galaxies ($M_r \sim -18$) are mostly blue, while large galaxies are generally redder. Furthermore, galaxies with large velocity distributions are mostly massive and vise versa. The tendency agrees with the observational results from SDSS.

Keywords: galaxies: luminosity function, mass function – galaxies: halos – dark matter

1 Introduction

Various studies have studied the luminosity function (LF) of galaxies (e.g., Press & Schechter, 1974; Schechter, 1976; Blanton et al., 2003, 2005b). Observationally, the LF can be easily obtained from the simplest photometric measurements and regarded as a direct probe of the galactic stellar mass.

Apart from observations, simulations has now become another powerful tool to study the mystery of galaxies (e.g., Vogelsberger et al., 2014; Wetzel et al., 2016; Pillepich et al., 2018; Hopkins et al., 2018). A competitive advantage of simulations is that they allow us to study the universe in three-dimensions. Simulations also provide vast more sample galaxies with resolution down to the scale of star clusters. However, due to lack of knowledge of the sub-grid

*Email: ybchen@umich.edu
†UMID: *54095800*
‡Double spacing is not very good looking... So I still stick on single spacing.

physics like star formation and sub-grid feedback, simulations can hardly reproduce exactly the observational results like the LF (Vogelsberger et al., 2013, e.g.,).

In this work, I compare the observational results of the LF with a state-of-art simulation, and investigate different mass distributions of galaxies with different colors and velocity dispersions. I also analyze the limitations of simulations qualitatively. The rest of the paper is organized as below. In Sec. 2, I describe my methodology in greater detail. I then post my major results in Sec. 3. Finally, I summarize the key points of this work in Sec. 4.

2 Method

2.1 IllustrisTNG

The cosmological simulation, IllustrisTNG (Pillepich et al., 2018)[1], is performed with the moving-mesh quasi-Lagrange code, AREPO (Springel, 2010). This suite has three groups of simulations with different sizes of simulation boxes. Since TNG50 is unpublished yet, I use TNG100 (box side-length ~ 100 Mpc) and TNG300 (box side-length ~ 300 Mpc) simulations in this work. TNG100 (TNG300) initially has 2×1820^3 (2×2500^3) particles, respectively, and can thus resolve a minimum mass scale of $10^6\ M_\odot$ ($10^7\ M_\odot$). The TNG simulations apply the Planck16 cosmology (Planck Collaboration et al., 2016), i.e., a flat ΛCDM cosmology with $\Omega_\mathrm{m} = 0.3089$, $\Omega_\mathrm{b} = 0.0486$, $\Omega_\Lambda = 0.6911$, $h = 0.6774$, $n_s = 0.9667$, and $\sigma_8 = 0.8519$. The simulations start at $z = 127$, and evolve to the present ($z = 0$), producing 100 snapshots. The TNG suite also includes realistic baryon physics, enabling analysis on stellar statistics.

2.2 NYU-VAGC

I collect observational data of low-redshift galaxies, including absolute magnitudes, Petrosian half-light surface brightness, etc., form the New York University Value-Added Galaxy Catalog (NYU-VAGC, Blanton et al., 2005a) [2] based on the Sloan Digital Sky Survey (SDSS, Abazajian et al., 2003). The low-redshift dataset of NYU-VAGC covers 2221 deg^2 of the sky in the range, $10\ h^{-1}\,\mathrm{Mpc} < d < 150\ h^{-1}\,\mathrm{Mpc}$. NYU-VAGC has 49967 galaxies in total with valid r-band absolute magnitudes, which are K-corrected to fix the bias caused by redshift.The detectability is limited to a maximum r-band apparent magnitude, $r < 17.7$. Therefore, a volume correction is also applied in this work (see Mid-term Project 2).

[1] `https://www.tng-project.org/`
[2] `https://sdss.physics.nyu.edu/vagc/`

3 Results

3.1 Galaxy Luminosity Function

The halo catalog of TNG is obtained with the FOF algorithm based on the fragmentation of dark matter. Each FOF halo is then divided by several (or one or even zero) subhalos by the SUBFIND algorithm (Springel et al., 2001). A subhalo is a gravitationally bound system with a galaxy embedded in the center. The SDSS-filtered magnitudes are given from the stellar components of a simulated galaxy.

The Gaussian kernel density estimation (KDE) is employed in replace of the traditional histogram method. The KDE method includes the information of every samples and produces smoother curves, making it a better method here to illustrate the galaxy LF. The Gaussian KDE method view each galaxy as a Gaussian distribution in the M_r space, and the summation of all Gaussian distributions can be regarded as an estimation of the real LF of galaxies. The width, h, of the Gaussian kernel is arbitrary, but does not significantly affect the results. For simplicity, I use $h = 0.2$ dex (the kernel width is the two times standard deviation of Gaussian distribution) for the KDE here.

The LFs from simulation, observation, and theoretical fitting by Blanton et al. (2005a) are shown in Fig. 1. The LFs are based on low-redshift galaxies with $z \approx 0$. For simulations, the LFs are consistent with the observation at $-21 < M_r - 5\log_{10} h < -16$, but are flatter at both bright and faint ends. That is, simulated galaxies tend to be brighter than reality. Additionally, the LF of TNG300 is systematically smaller than that of TNG100. This is because the resolution of TNG300 is ~ 10 times lower than TNG100, which leads to less identified halos/subhalos (see Vogelsberger et al., 2013). However, this effect only swift the magnitude of LFs, but only slightly change the shape except for the faintest end.

3.2 Luminosity Functions of Galaxies with Different Colors

The color distribution of galaxies show clear bimodality (see Blanton & Moustakas, 2009, and Fig. 1 in Mid-term Project 2). I find that the two peaks can be well distinguished by the threshold of $g - r = 0.6$. Therefore, I divide all galaxies into blue ($g - r < 0.6$) and red ($g - r > 0.6$) galaxies, and plot the LFs for both components in Fig. 2. As for the observational results, median and small size galaxies ($M_r \sim -17$) are mostly blue, while large galaxies are generally redder. However, the faintest galaxies again tend to have sightly more red components than the median size galaxies. Such tendency agrees with simulations, but the shift from red-domination to blue-domination is at brighter end for the TNG suite. This reveals the active nature of median size galaxies. Due to lack of baryons at the faint end and strong feedback at the bright end, only median size galaxies can form stars effectively at low redshift, resulting in a blue-domination at this luminosity range.

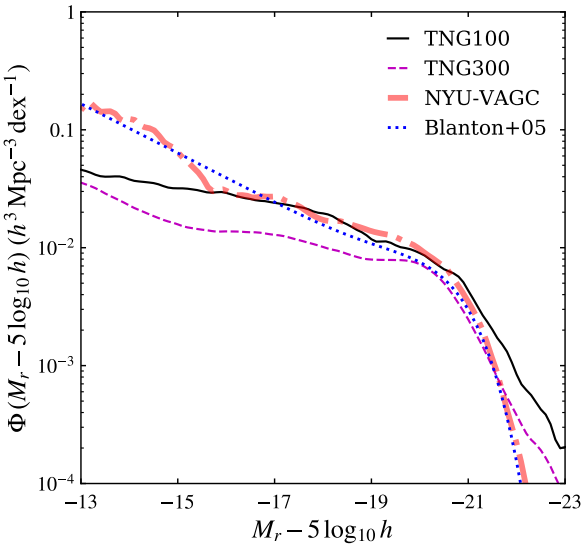

Figure 1: Luminosity functions of galaxies from TNG100 (black solid), TNG300 (magenta dashed), and NYU-VAGC (red dot-dashed). The double-Schechter fitting given by Blanton et al. (2005a) is also plotted (blue dotted). Note that the observational curve from NYU-VAGC is already volume corrected for $M_r - 5\log_{10}h > -17.7$.

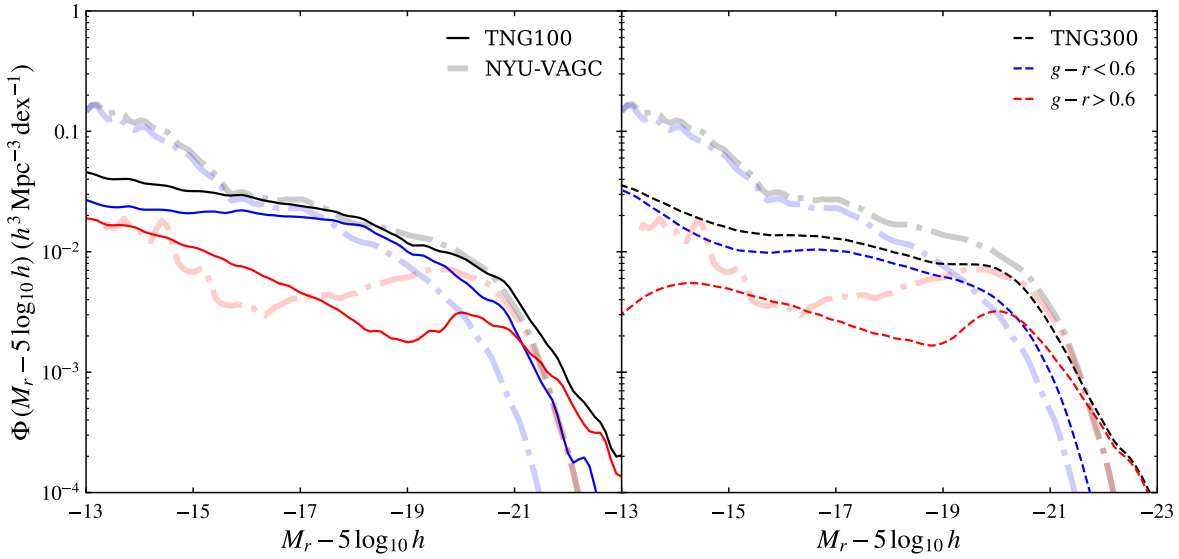

Figure 2: Left: luminosity functions of galaxies with $g - r < 0.6$ (blue) and $g - r > 0.6$ (ref) from TNG100; right: the same for TNG300. The total LFs, i.e., the summation of blue and red curves, are shown in black curves. The background is the observational LFs from NYU-VAGC, also divided into blue and red components.

3.3 Luminosity Functions of Galaxies with Different Velocity Dispersions

The velocity dispersion harder to measure in observations, but easy to get via simulations. To study mass distributions of galaxies with different velocity dispersion, I divide all galaxies into low-velocity dispersion ($\sigma < 70$ km s^{-1}) and high-velocity dispersion ($\sigma > 70$ km s^{-1}) components, and plot their LFs in Fig. 3. However, the observed LFs now deviate significantly with the simulated ones. As for observations, the behavior of low-velocity dispersion galaxies are similar to blue galaxies, while high-velocity dispersion galaxies are similar to red galaxies, see Fig. 2. This is because redder (older) stars have experienced stronger relaxation, evolved off the original orbits, and gained more random motions. Nevertheless, almost all simulated bright galaxies have high-velocity dispersion, and nearly no bright galaxies with $M_r < -20$ have velocity dispersion lower than 70 km s^{-1}. Although brighter galaxies do have systematically higher velocity dispersion, it makes no sense that faint galaxies all have low velocity dispersion. I suggest that this is because the sub-grid model of simulations is oversimplified. The kinematics of baryon particles is too strongly influenced by the host dark matters, resulting in underestimated scatter in the $\sigma - M_r$ space.

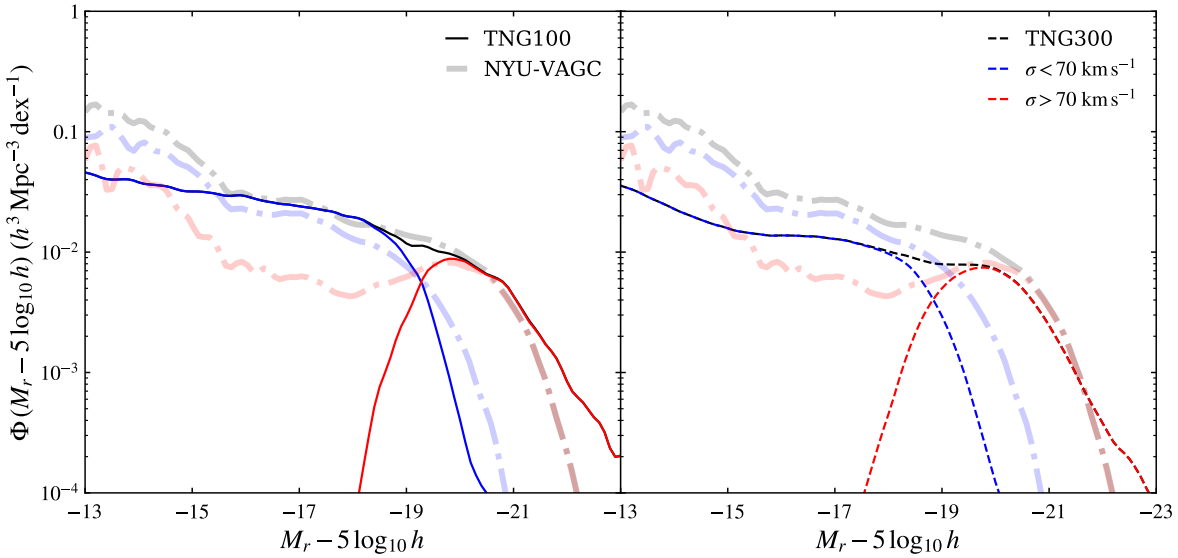

Figure 3: Left: luminosity functions of galaxies with $\sigma < 70$ km s^{-1} (blue) and $\sigma > 70$ km s^{-1} (ref) from TNG100; right: the same for TNG300. The total LFs, i.e., the summation of low and high-velocity dispersion curves, are shown in black curves. The background is the observational LFs from NYU-VAGC, also divided into low and high-velocity dispersion components.

4 Summary

In this work, I produce the LF of low-redshift galaxies with the hydrodynamic cosmological simulation, IllustrisTNG, and compare it the observational results from NYU-VAGC. I find

that simulated galaxies tend to be more massive with flatter LFs. Both simulations and observations reveal a red-domination at the bright end, and a blue-domination at the median size range of $M_r \sim 18$. Due to lack of baryons at the faint end and strong feedback at the bright end, median size galaxies tend to have more younger stellar populations, and thus bluer. For the same reason, the observed velocity dispersion of median size galaxies is also lower than the that of the faint end and largely lower than the bright end. However, the simulated galaxies tend to have too small scatter in the $\sigma - M_r$ space. I suggest that this is because the influence of dark matter on baryon matter is over estimated.

5 Supplementary Materials

Source code of this work can be found in `https://github.com/EnthalpyBill/ASTRO533/tree/master/project_final`.

Acknowledgment

I thank Mark Vogelsberger for providing the IllustrisTNG data. I also thank Mayura Balakrishnan, Eric Bell, William Kevin Black, Anne Blackwell, Rory Patrick Bowens, Paul Draghis, Andrew Zane Gardner, Katya Gozman, Nour Ibrahim, Lena Komarova, Isaac Malsky and Dante Leonardo Vozza for getting up by 8:30 am and giving constructive discussions.

References

Abazajian K., et al., 2003, AJ, 126, 2081

Blanton M. R., Moustakas J., 2009, Annu. Rev. Astron. Astrophys., 47, 159

Blanton M. R., et al., 2003, ApJ, 592, 819

Blanton M. R., et al., 2005a, AJ, 129, 2562

Blanton M. R., Lupton R. H., Schlegel D. J., Strauss M. A., Brinkmann J., Fukugita M., Loveday J., 2005b, ApJ, 631, 208

Hopkins P. F., et al., 2018, MNRAS, 480, 800

Pillepich A., et al., 2018, MNRAS, 475, 648

Planck Collaboration et al., 2016, A&A, 594, A13

Press W. H., Schechter P., 1974, ApJ, 187, 425

Schechter P., 1976, ApJ, 203, 297

Springel V., 2010, MNRAS, 401, 791

Springel V., White S. D. M., Tormen G., Kauffmann G., 2001, MNRAS, 328, 726

Vogelsberger M., Genel S., Sijacki D., Torrey P., Springel V., Hernquist L., 2013, MNRAS, 436, 3031

Vogelsberger M., et al., 2014, Nature, 509, 177

Wetzel A. R., Hopkins P. F., Kim J.-h., Faucher-Giguère C.-A., Kereš D., Quataert E., 2016, ApJ, 827, L23